Biosensors and Bioelectronics 54 (2014) 217–221

Contents lists available at ScienceDirect

Biosensors and Bioelectronics

journal homepage: www.elsevier.com/locate/bios

Short communication

Aptamer biosensor for sensitive detection of toxin A of *Clostridium difficile* using gold nanoparticles synthesized by *Bacillus stearothermophilus*

Peng Luo [a,*,1], Yi Liu [b,1], Yun Xia [a], Huajian Xu [a], Guoming Xie [c]

[a] Clinical Laboratory, The First Affiliated Hospital, Chongqing Medical University, Chongqing 400016, PR China
[b] Department of Medical Technique, Chongqing Medical and Pharmaceutical College, Chongqing 400030, PR China
[c] Key Laboratory of Medical Diagnostics of Ministry of Education, Chongqing Medical University, Chongqing 400016, PR China

ARTICLE INFO

Article history:
Received 15 August 2013
Received in revised form
20 October 2013
Accepted 4 November 2013
Available online 12 November 2013

Keywords:
Clostridium difficile
Toxin
Aptamer
Biosynthesis
Nanoparticles
Biosensor

ABSTRACT

A sensitive electrochemical biosensor was developed to detect toxin A (TOA) of *Clostridium difficile* based on an aptamer selected by the systematic evolution of ligands using exponential enrichment and gold nanoparticles (GNPS) synthesized by *Bacillus stearothermophilus*. The thiolated single-stranded DNA used as the capture probe (CP) was first self-assembled on a Nafion–thionine–GNPS-modified screen-printed electrode (SPE) through an Au–thiol interaction. The horseradish peroxidase (HRP)-labeled aptamer probe (AP) was then hybridized to the complementary oligonucleotide of CP to form an aptamer–DNA duplex. In the absence of TOA, the aptamer–DNA duplex modified the electrode surface with HRP, so that an amperometric response was induced based on the electrocatalytic properties of thionine. This was mediated by the electrons that were generated in the enzymatic reaction of hydrogen peroxide under HRP catalysis. After the specific recognition of TOA, an aptamer–TOA complex was produced rather than the aptamer–DNA duplex, forcing the HRP-labeled AP to dissociate from the electrode surface, which reduced the catalytic capacity of HRP and reduced the response current. The reduction in the response current correlated linearly with the concentration of TOA in the range of 0–200 ng/mL. The detection limit was shown to be 1 nM for TOA. This biosensor was applied to the analysis of TOA and showed good selectivity, reproducibility, stability, and accuracy.

© 2013 Elsevier B.V. All rights reserved.

1. Introduction

Clostridium difficile is one of the predominant pathogens involved in nosocomial intestinal infections, and can cause antibiotic-associated diarrhea and pseudomembranous colitis in humans and animals (Rupnik et al., 2009; Friedman et al., 2013). This organism produces at least two toxins, designated toxins A and B (Lyerly et al., 1982). Toxin A (TOA) is the lethal enterotoxin, and can cause hemorrhage and fluid secretion. Toxin B (TOB) is an extremely potent cytotoxin for many cultured cells. The incidence of *C. difficile* infection (CDI) is increasing throughout the world with the universal use of antibiotics (Depestel and Aronoff (2013); Varughese et al., 2013). A rapid and sensitive diagnosis can contribute to the timely treatment of patients and to the control of the nosocomial spread of these infections (Gerding et al., 2008; Barbut et al., 2005). Currently, the primary laboratory tests used for a presumptive diagnosis of CDI involve the detection of the organism, TOA, or TOB in stool samples (Kyne et al., 2000; Bartlett and Gerding (2008)). Although microbiological culture is the traditional method for determining CDI (George et al., 1979), it is usually both insensitive and time-consuming. A cytotoxic assay based on the cytopathic effect of the bacterium on tissue-culture cells is regarded as the reference method for the diagnosis of CDI, but this assay is costly and slow, and requires some expertise (Aldeen et al., 2000). An enzyme immunoassay has been used to detect CDI in many clinical studies (Musher et al., 2007). However, some antibodies can cross-react, leading to false positive results in these enzyme-linked immunosorbent assay (ELISA)-based tests. Polymerase chain reaction (PCR) should be a rapid and sensitive diagnostic method, but small amounts of free DNA in a sample would reduce the positive detection rate, and laborious sample pretreatment would also affect its accuracy (Van den Berg et al. (2007)).

To overcome these limitations, new recognition elements for bioassays are attracting increasing interest. An aptamer is a synthetic single-stranded DNA or RNA oligonucleotide that can specifically bind to target molecules, such as nucleic acids, proteins, cells, and other organic or inorganic molecules (Shangguan et al., 2006). Aptamers have many significant advantages compared with antibodies,

* Corresponding author. Tel.: +86 23 89012352.
E-mail address: nclp261@163.com (P. Luo).
[1] These authors contributed equally to this work.

0956-5663/$ - see front matter © 2013 Elsevier B.V. All rights reserved.
http://dx.doi.org/10.1016/j.bios.2013.11.013

including their high affinity, low immunogenesis, fast tissue penetration rate, and low molecular weight (Ray et al., 2012). They can be chemically synthesized at low cost and easily modified with a variety of chemical groups, including fluorescent dyes, biotin, thiols, and enzymes (Yang et al., 1998). The assumption can be made that an aptamer can recognize a molecular target such as TOA, and can therefore provide a useful early assay for the identification of CDI.

Recently, biosensors based on aptamers have gained much attention in biochemical analyses (Zhang et al., 2011), clinical diagnoses (Kim et al., 2011), food quality control (Chen et al., 2012), and environmental monitoring (Goda and Miyahara (2012)). Therefore, they seem to be excellent candidates for the rapid and sensitive diagnosis of TOA.

At present, gold nanoparticles (GNPS) have been widely used in the preparation of biosensors because of their excellent electron transfer ability and strong adsorptive capacity (Singh et al., 2013; Rawal et al., 2012; Bertok et al., 2013; Meng et al., 2012). Moreover, there is a growing need to develop environmentally friendly processes for GNPS synthesis that do not use toxic chemicals. Therefore, the microbial synthesis of GNPS has attracted much interest because many microorganisms can strongly adsorb metal ions and reduce them to metal nanoparticles with properties similar to those of chemically synthesized materials (Fayaz et al., 2011; Rajasree and Suman (2012); Thirumurugan et al., 2012). In this paper, we report the first attempt to use *Bacillus stearothermophilus*, a Gram-positive bacterium that rarely causes disease in healthy people, to synthesize GNPS that can immobilize thiolated single-stranded DNA through an Au–thiol interaction.

We describe a novel disposable biosensor for TOA based on the structural switching of an aptamer. In the absence of TOA, the aptamer–DNA duplex formed by the hybridization reaction between the capture probe (CP) and the aptamer probe (AP) induces a clear enzymatic catalysis of the oxidation of thionine by hydrogen peroxide. The addition of TOA induces a conformational change in the aptamer, resulting in the formation of an aptamer–TOA complex, which causes the dissociation of the HRP-labeled AP from the electrode surface, lowering the response current. The reduction in the response current depends only on the concentration of TOA, and this characteristic is the basis of the biosensor designed for the quantitative analysis of TOA. The analytical performance of and optimal conditions for this biosensor were investigated. Under optimal conditions, the biosensor response to TOA shows good selectivity, reproducibility, stability, and accuracy. The proposed aptasensor was used to measure TOA in stool samples and satisfactory results were obtained.

2. Experimental

2.1. Reagents and apparatus

All oligonucleotides were chemically synthesized by Sangon Biotechnology Co., Ltd (Shanghai, China). Their sequences are listed in Table SI1 of the Supplementary information. Toxin A, Nafion-117 solution, thionine, magnetic beads, chlorauric acid ($HAuCl_4$), and 6-mercaptohexanol (MCH) were purchased from Sigma-Aldrich (Shanghai, China). Carbon ink, silver ink, and UV adhesives were purchased from TaiTungHong (ShenZhen, China). *C. difficile* and *B. stearothermophilus* were gifts from the First Affiliated Hospital of Chongqing Medical University. All other reagents were of analytical grade and used without further purification. All of the solutions were prepared with ultrapure water from a Millipore Milli-Q system.

Cyclic voltammetric analysis and electrochemical impedance spectroscopy were performed with a CHI-660D workstation (Chenhua, China). A transmission electron microscope (Phillips, Netherlands), ultraviolet–visible spectrophotometer (Persee, China), flow cytometer (BD, USA), PCR thermocycler (ABI, USA), microplate reader (Tecan, Switzerland), and a screen printer (Shengjiang, China) were used.

2.2. Preparation of the aptasensor

The detailed procedures for the selection of the aptamer and the preparation of GNPS are given in the 'Experimental' section of the Supporting information. The screen-printed electrode (SPE) with a carbon working electrode (WE; diameter, 3 mm), carbon counter electrode, and Ag/AgCl reference electrode was fabricated according to the literature (Yu et al., 2004; Luo et al., 2008). The aptasensor was developed with the following steps. WE was rinsed thoroughly with ultrapure water and dried at room temperature. Nafion-117 solution (5%, w/w) was diluted to 1% (w/w) with absolute ethanol; 10 μL of 1% (w/w) Nafion was dropped onto the WE surface and allowed to dry in air at room temperature; 10 μL of 1 mmol/L thionine (pH 6.5) was dropped onto the Nafion-modified electrode and allowed to stand for 1 h at room temperature. After the Nafion–thionine-modified electrode was rinsed thoroughly with ultrapure water, it was immersed in 20 ml of GNPS solution for 2 h at room temperature with vigorous stirring. The pretreated electrode was rinsed with ultrapure water again, and 10 μL of 100 nM CP solution was dripped onto the surface of the Nafion–thionine–GNPS-modified electrode for 1 h at 37 °C. The electrode surface was then passivated with 1 mM of MCH for 1 h. The electrode surface was washed with ultrapure water to remove any unbound oligonucleotide. Following these procedures, the Nafion–thionine–GNPS–CP-modified electrode was immersed in 100 nM HRP-labeled AP solution to hybridize for 1 h at 37 °C. After thorough rinsing, the biosensor was ready.

2.3. Electrochemical measurements

Phosphate-buffered saline (PBS; 25 μL at pH 7.0) containing 5.0 mM H_2O_2 was dropped onto the biosensor surface without stirring. The electrochemical signals were obtained using cyclic voltammetry (CV) with a potential range from –0.1 V to –0.5 V (vs Ag/AgCl) at a scanning rate of 20 mV/s.

3. Results and discussion

3.1. Characterization of the aptamer

The in vitro selection and amplification of the aptamer are described in the section 'Results and discussion' of the Supporting information. The binding of the aptamer to the target was monitored directly with flow cytometry. The selected aptamers were labeled with fluorescein isothiocyanate (FITC) and incubated with TOA. The fluorescence intensity measured with flow cytometry represented the binding capacity of the aptamer for TOA. After incubation with TOA, the fluorescence intensity shifted to the right relative to that of the FITC–aptamer, suggesting a significant increase in the fluorescence intensity (Fig. SI3). These results indicate that the aptamer directed against TOA can bind to the target protein. Because aptamers can be regarded as "shape libraries", the potential secondary structure of the selected sequence was predicted using the DNAMan software. As shown in Fig. SI4, two stable stem–loop structures, each composed of about eight bases, were formed and the relative free energy was –4.00. Based on these results, we considered that the selected aptamer bound TOA of *C. difficile* because of its sequence and structural conformation.

3.2. Characterization of GNPS

The gold nanoparticles were examined by transmission electron microscopy (TEM). As shown in Fig. 1, differently shaped particles, including spherical, triangular, and other shapes, were observed, with diameters of approximately 5–30 nm. The TEM images confirmed that GNPS were produced. A possible explanation of this phenomenon is that enzymes secreted by *B. stearothermophilus* reduce Au^{3+} to Au^{0}, with the consequent formation of GNPS. Fig. SI5 shows the UV–visible spectra of GNPS synthesized with the chemical method (curve a) and with the microbial method (curve b). As shown in Fig. SI5, the GNPS showed a characteristic plasmon resonance band at 530 nm, indicating the presence of gold particles with nanoscale dimensions (Silvestrini and Ugo (2013)). However, the λ_{max} of the GNPS synthesized by the microbial method exhibited a red shift compared with the λ_{max} of the GNPS synthesized with the chemical method, indicating that the gold particles synthesized by the microbial method were larger than those synthesized chemically. This result is consistent with that reported in the literature (Jin et al., 2007). GNPS produced by *B. stearothermophilus* were used throughout the experiment.

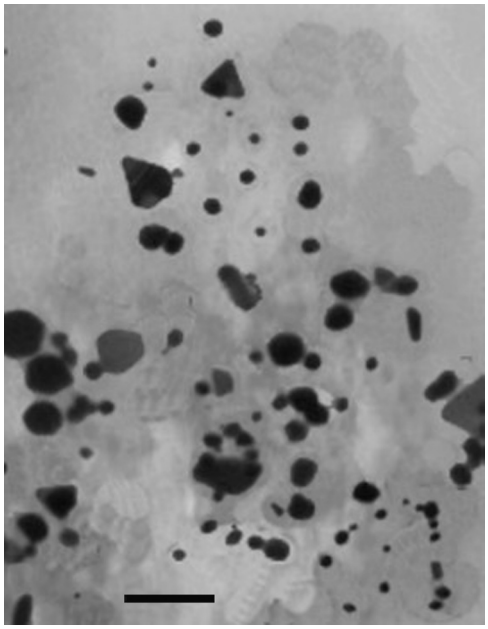

Fig. 1. TEM image of GNPS synthesized by *B. stearothermophilus* (scale bar=50 nm).

3.3. Principle of the electrochemical aptasensor

Fig. 2 illustrates the principle of the electrochemical biosensor for TOA based on an AP probe and an enzymatic amplification protocol. The thiolated CP was first immobilized on a Nafion–thionine–GNPS-modified SPE through an Au–thiol interaction. The HRP-labeled AP was then modified on the electrode surface by hybridizing it with CP to form an aptamer–DNA duplex (Fig. 2A). Without TOA, the HRP attached to the electrode could catalyze the oxidation of thionine by hydrogen peroxide. As shown in Fig. 2C, the oxidized form of HRP, which was produced in the reaction with hydrogen peroxide, was reduced by the thionine immobilized on the Nafion film. The thionine was reduced electrochemically on the electrode. With the addition of the target (TOA), the binding of the aptamer to TOA produced an aptamer–TOA complex, replacing the aptamer–DNA complex, and causing the dissociation of the HRP-labeled AP from the electrode (Fig. 2B). This reduced the catalytic capacity of HRP and consequently the response current. Because the concentrations of thionine and hydrogen peroxide were constant, the reduction in the response current depended only on the concentration of TOA. This characteristic was used as the basis of the biosensor design for the detection of TOA.

3.4. Electrochemical behavior of the aptasensor

Cyclic voltammograms of the aptasensor were recorded and are shown in Fig. 3. No obvious peak current was observed for the bare SPE or the Nafion-modified electrode because there was no electron mediator (curves a and b). However, in the voltammogram obtained for the Nafion–thionine-modified electrode (curve c), a symmetrical anodic and cathodic peak was observed, which showed that a quasireversible redox reaction occurred at the electrode. A possible explanation is that thionine can be absorbed by Nafion through ion exchange and performs well as an electron mediator (Moretto et al., 2013; Ou et al., 2007). The peak currents increased dramatically after GNPS were introduced into the Nafion–thionine film (d). This can be attributed to the GNPS, which act as electron-conducting tunnels to facilitate electron transfer (Guo and

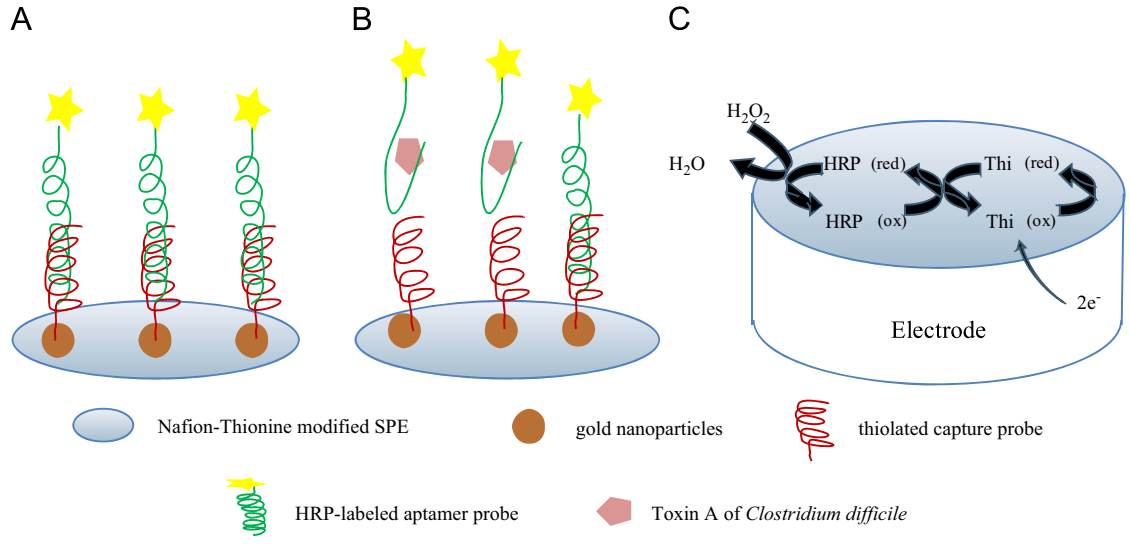

Fig. 2. Schematic representation of the aptasensor for TOA. (A) HRP-labeled aptamer probe hybridizes with the complementary part of the capture probe, (B) HRP-labeled aptamer probe recognizes toxin A, and (C) the enzymatic mechanism based on HRP reactivity for H_2O_2.

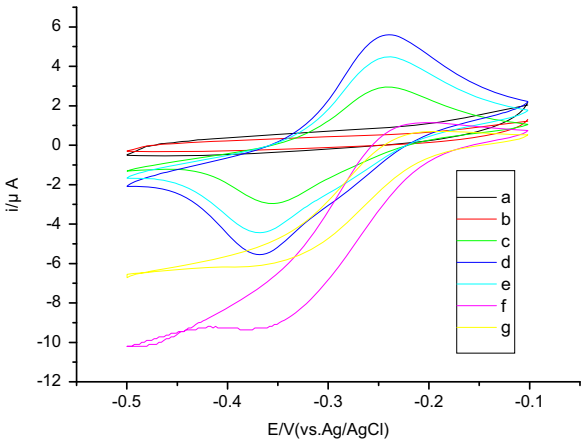

Fig. 3. CV curves for different electrodes in PBS (pH 7.0) with 5.0 mM H_2O_2 at a scan rate of 20 mV/s: (a) bare SPE, (b) Nafion, (c) Nafion–thionine, (d) Nafion–thionine–GNPS, (e) Nafion–thionine–GNPS–CP, (f) Nafion–thionine–GNPS–CP–AP, and (g) Nafion–thionine–GNPS–CP–AP–TOA.

Wang (2007)). However, the peak currents decreased after CP was immobilized onto the Nafion–thionine–GNPS-modified electrode (e). A possible reason is that GNPS can covalently immobilize an aptamer modified with a thiol group via Au–S bonding, and the CP immobilized in the composite film can partly hinder electron transfer. The modified biosensor was then hybridized with the HRP-labeled AP, which caused a great reduction in the oxidation peak current and a sharp increase in the reduction peak current (f). These results clearly indicate the presence of the HRP-labeled AP on the biosensor interface and that the peak current response derives from the electrocatalytic property of the HRP on the electrode surface. After the aptasensor reacted with TOA, the reduction peak current decreased further (g), because the introduction of the target induces a structural switch in the aptamer, resulting in the dissociation of the HRP-labeled AP from the electrode surface and the simultaneous decline in the peak current intensity. These results are consistent with the electrochemical impedance spectroscopy shown in Fig. SI6.

3.5. Optimization of surface coverage

The immobilized CP had a profound effect on the aptasensor surface coverage, because the lower densities had a limited number of biorecognition sites, whereas the higher surface densities resulted in steric and electrostatic interference between the probes and the aptamer. Therefore, the effects of different concentrations of CP on the response current of the aptasensor were investigated. The measurements were made according to the following procedure: 10 μL of different concentrations of CP solution (10, 50, 100, 150, or 200 nM) were dripped onto the surface of the Nafion–thionine–GNPS-modified electrode. Then, 25 μL of PBS (pH 7.0) without H_2O_2 was dropped onto this modified electrode and the response current was recorded. As shown in Fig. SI7A, as the concentration of CP increased, the response current decreased and leveled off slowly at concentrations of up to 100 nM. This shows that the surface was saturated with CP at this concentration. Although 10 nM CP produced the highest current intensity, 100 nM was selected as the optimal CP concentration based on the principle that a higher concentration of probe can better hybridize to the target sequence.

Because the hybridization of CP and AP is the key factor producing the high current intensity in the absence of the target, the optimal AP concentration was then assessed experimentally by varying the AP concentration in the range of 10–200 nM. The measurements were made according to the following procedure. The Nafion–thionine–GNPS–CP-modified electrode was immersed in different concentrations of HRP-labeled AP solution (10, 50, 100, 150, or 200 nM) to hybridize with CP. Then, 25 μL of PBS (pH 7.0) with H_2O_2 was dropped onto this modified electrode and the response current was recorded. As shown in Fig. SI7B, the current increased as the AP concentration increased up to 100 nM, and then started to plateau. This result indicates that the surface of the probe-modified electrode was saturated. Thus, 100 nM was selected as the optimal AP concentration for this study.

3.6. Quantitative measurement of TOA

Under the optimal conditions (provided in the Supporting information), TOA was quantified using the aptasensor by introducing increasing concentrations of TOA. Fig. SI9 shows that with increasing amounts of TOA, the response current decreased gradually and began to level off when the TOA concentration was about 300 ng/mL. As shown in the inset of Fig. SI9, the current increment (Δi) correlated linearly with the concentration of TOA in the range of 0–200 ng/mL. The calibration equation obtained from this curve was $\Delta i = 0.03C + 0.1$ (where C is the TOA concentration), with a linear slope of 0.03 and a correlation coefficient of 0.9993. The detection limit was calculated as 1 ng/mL according with the 3SD/K criterion, where K is the slope of the calibration graph and SD is the standard deviation ($n=3$) of the signals in the blank samples.

3.7. Selectivity, precision, stability, and accuracy

Because selectivity is important in practical applications of the aptasensor, other toxins, such as TOB of *C. difficile*, *Shiga* toxin, and *Botulinum* toxin, were used to evaluate the selectivity of the aptasensor. The concentration of TOA used was 50 ng/mL, whereas the concentrations of the other toxins were 100 ng/mL in the selectivity experiment. As shown in Fig. SI10, the signals for *Shiga* toxin and *Botulinum* toxin were close to the signal for TOA. However, the presence of TOB caused a notable increase in the response current. A possible reason is that the N-terminal amino acids of TOB are 64% homologous to those of TOA, which can result in TOB combined with aptamer of TOA. Although TOB produced by *C. difficile* could affect the detection of TOA, the presence of TOB could also demonstrate a *C. difficile* infection, and could contribute to a reduction in the number of missed diagnoses. These results suggest that the aptasensor developed here can detect *C. difficile* infections with good selectivity.

The precision and reproducibility of disposable biosensors are key factors in their construction and application. To test the precision and reproducibility of the present aptasensor, 10 different disposable aptasensors, developed independently, were used to test 10 different samples with the same TOA concentration (50 ng/mL), and a relative standard deviation of 4.8% was obtained, showing the acceptable detection precision. The aptasensor showed good stability during storage, with 87.6% of its original response remaining after storage for 2 weeks at 4 °C in PBS (pH 7.0).

Recovery tests were used to evaluate the accuracy of the aptasensor in practical applications. Three TOA samples of different concentrations were first analyzed with an ELISA. The samples were then assayed with the aptasensor. Table SI2 shows the concentrations found and the recoveries obtained with the aptasensor. The aptasensor showed good recovery values. These results suggest that the biosensor can be used to assay TOA in fecal samples with high accuracy.

4. Conclusion

In this study, a novel disposable TOA aptasensor with high sensitivity was developed. The experimental results demonstrate that the proposed method may be a valuable screening procedure for CDI and can be readily extended to the detection of other clinically important antigens. However, the aptasensor cannot effectively discriminate between TOA and TOB because their amino acid structures are similar. Therefore, an anti-TOA aptamer with a greater recognition capacity will be developed in a future study.

Acknowledgments

This work was supported by the Research Foundation of Chongqing Municipal Health Bureau, China (2012-2-023) and the Research Program of Chongqing Medical and Pharmaceutical College, China (2010103).

Appendix A. Supplementary material

Supplementary data associated with this article can be found in the online version at http://dx.doi.org/10.1016/j.bios.2013.11.013.

References

Aldeen, W.E., Bingham, M., Aiderzada, A., Kucera, J., Jense, S., Carroll, K.C., 2000. Diagn. Microbiol. Infect. Dis 36, 211–213.
Barbut, F., Decre, D., Lalande, V., Burghoffer, B., Noussair, L., Gigandon, A., Espinasse, F., Raskine, L., Robert, J., Mangeol, A., Branger, C., Petit, J.C., 2005. J. Med. Microbiol. 54, 181–185.
Bartlett, J.G., Gerding, D.N., 2008. Clin. Infect. Dis. 46 (suppl 1), S12–S18.
Bertok, T., Sediva, A., Katrlik, J., Gemeiner, P., Mikula, M., Nosko, M., Tkac, J, 2013. Talanta 108, 11–18.
Chen, J.H., Fang, Z.Y., Liu, J., Zeng, L.W., 2012. Food. Control 25, 555–560.
Depestel, D.D., Aronoff, D.M., 2013. J. Pharm. Pract. 26, 464–475.
Fayaz, A.M., Girilal, M., Rahman, M., Venkatesan, R., Kalaichelvan, P.T., 2011. Process. Biochem. 46, 1958–1962.
Friedman, N.D., Pollard, J., Stupart, D., Knight, D.R., Khajehnoori, M., Davey, E.K, Parry, L., Riley, T.V., 2013. BMC. Infect. Dis. 13, 459–463.
George, W.L., Sutter, V.L., Citron, D., Finegold, S.M., 1979. J. Clin. Microbiol. 9, 214–219.
Gerding, D.N., Muto, C.A., Owens, R.C., 2008. Clin. Infect. Dis. 46 (suppl 1), S43–S49.
Goda, T., Miyahara, Y., 2012. Biosens. Bioelectron. 32, 244–249.
Guo, S., Wang, E., 2007. Anal. Chim. Acta 598, 181–192.
Jin, Y., Wang, P.J., Yin, D.H., Liu, J.F., Qin, L.S., Yu, N.Y., Xie, G.Y., Li, B.M., 2007. Colloid Surf. A 302, 366–370.
Kim, J.P., Kwon, I.K., Sim, S.J., 2011. Biosens. Bioelectron. 26, 4823–4827.
Kyne, L., Warny, M., Qamar, A., Kelly, C.P., 2000. N. Engl. J. Med. 342, 390–397.
Luo, P., Liu, Y., Xie, G.M., Xiong, X.L., Deng, S.X., Song, F.Z., 2008. Forensic Sci. Int. 179, 192–198.
Lyerly, D.M., Lockwood, D.E., Richardson, S.H., Wilkins, T.D., 1982. Infect. Immun. 35, 1147–1150.
Meng, X.M., Xu, M.R., Zhu, J.Y., Yin, H.S., Ai, S.Y, 2012. Electrochim. Acta 71, 233–238.
Moretto, L.M., Montagner, F., Ganzerla, R., Ugo, P., 2013. Anal. Bioanal. Chem. 405, 3603–3610.
Musher, D.M., Manhas, A., Jain, P., Nuila, F., Waqar, A., Logan, N., Marino, B., Graviss, E.A., 2007. J. Clin. Microbiol. 45, 2737–2739.
Ou, C.F., Yuan, R., Chai, Y.Q., Tang, M.Y., Chai, R., He, X.L., 2007. Anal. Chim. Acta 603, 205–213.
Rajasree, S.R.R., Suman, T.Y., 2012. Asian. Pac. J. Trop. Med. 2, S796–S799.
Rawal, R., Chawla, S., Pundir, C.S., 2012. Biosens. Bioelectron. 31, 144–1450.
Ray, P., Rialon, G.K.L., Veras, E., Sullenger, B.A., White, R.R, 2012. J. Clin. Invest. 122, 1734–1741.
Rupnik, M., Wilcox, M.H., Gerding, D.N., 2009. Nat. Rev. Microbiol. 7, 526–536.
Shangguan, D.H., Li, Y., Tang, Z.W., Cao, Z.C., Chen, H.W., Mallikaratchy, P., Sefah, K., Yang, C.Y.J., Tan, W.H, 2006. P. Natl. Acad. Sci. U.S.A. 103, 11838–11843.
Silvestrini, M., Ugo, P., 2013. Anal. Bioanal. Chem. 405, 995–1005.
Singh, S., Jain, D.V.S., Singl, M.L., 2013. Sensor. Actuat. B- Chem. 182, 161–169.
Thirumurugan, A., Ramachandran, S., Tomy, N.A., Jiflin, G.J., Rajagomathi, G., 2012. Korean. J. Chem. Eng. 29, 1761–1765.
Van den Berg, R.J., Vaessen, N., Endtz, H.P., Schulin, T., Van der Vorm, E.R., Kuijper, E.J., 2007. J. Med. Microbiol. 56, 36–42.
Varughese, C.A., Vakil, N.H., Phillips, K.M., 2013. J. Pharm. Pract. 26, 476–482.
Yang, Q., Goldstein, I.J., Mei, H.Y., Engelke, D.R., 1998. P. Natl. Acad. Sci. U.S.A. 95, 5462–5467.
Yu, H., Yan, F., Dai, Z., Ju, H.X., 2004. Anal. Biochem. 331, 98–105.
Zhang, J., Chen, P.P., Wu, X.Y., Chen, J.H., Xu, L.J., Chen, G.N., Fu, F.F., 2011. Biosens. Bioelectron. 26, 2645–2650.